

## Neutron transmutation doping of silicon: some experiments at the IEA-R1 research reactor

A. W. Carbonari, W. Pendl Jr. and R. N. Saxena

Instituto de Pesquisas Energéticas e Nucleares  
IPEN-CNEN/SP  
São Paulo, Brasil

### Abstract

An irradiation rig with simple design has been constructed and installed in the IEA-R1 research reactor for the neutron transmutation doping (NTD) of silicon with phosphorus. Crystal ingots with 3 and 4 inches diameter can be irradiated in this device. By adopting a procedure in which two ingots 20 cm long each are irradiated simultaneously and their positions interchanged at a point when precisely half the total necessary neutron dose has been received, it has been possible to achieve the desired axial uniformity of the neutron dose. This method avoids the use of neutron absorbing shields around the crystals which necessarily compromise the overall irradiation capacity of the reactor. Test irradiations were performed with 100 float zone silicon crystals and the results of radial and axial uniformities in the final resistivity values as well as the doping accuracy, obtained in the test irradiations show an excellent doping quality achieved.

### 1. INTRODUCTION

Pure silicon is the most common material used for the fabrication of electrical and electronic devices, ranging from large volume high voltage thyristors, power diodes and various types of transistors for medium to high power used in power plants, power transmission lines automotive control and power supplies to integrated circuits for computers and microprocessors. However, in order to be used in these devices, the silicon needs to be doped with another element to achieve the desired resistivity value which usually differs for different applications. The most commonly used dopants are phosphorus (for n-type silicon) and boron (for p-type silicon). The conventional phosphorus doping is carried out by the incorporation of the dopant in the required concentration in the molten stage during crystal growth. The conventional doping however leads to inhomogeneous distribution of the dopant due to segregation caused by low distribution coefficient of phosphorus in silicon and the resultant material presents large resistivity variations. As a consequence this material is unsuitable for the production of high volume devices such as rectifiers for high-voltage direct current (HVDC) transmission since the microscopic resistivity fluctuations (striations) may cause local break through ("hot spot") which not only have negative impact on device characteristics but they are usually detrimental to the device itself with eventual possibility of device breakdown.

The neutron transmutation doping (NTD) process is based on the capture of thermal neutrons by the  $^{30}\text{Si}$  nuclei (roughly 3.1% of silicon consists of  $^{30}\text{Si}$  isotope) producing the radioactive nuclei  $^{31}\text{Si}$  which decay with a half-life of 2.62 h to stable isotope of  $^{31}\text{P}$ , as is shown below:



The main advantage of using neutron transmutation doping results from the possibility to produce silicon with extremely homogeneous resistivity distribution since the irradiation of the silicon crystal can be performed in an homogeneous manner in nuclear reactors. The spreading resistance profile measurements have shown[1] that on a microscopic scale the total resistivity fluctuations of a conventionally doped float-zone silicon crystal could be as high as 30%. With neutron transmutation doping the resistivity variation can be reduced to less to 2-3%. Moreover since the neutron dose received by the silicon crystal during the irradiation can be determined with high accuracy, the resistivity targets can be achieved with very tight tolerance. The starting material is an undoped silicon crystal grown by the floating zone method. The main impurities are oxygen and carbon with typical concentrations in the range of  $10^{15}$  atoms/cm<sup>3</sup>. Metallic concentrations are below  $10^{10}$  atoms/cm<sup>3</sup>. Electrically active impurities are boron and phosphorous in the range of  $10^{12}$  atoms/cm<sup>3</sup>. Due to the excess of phosphorous in polycrystalline silicon, the undoped FZ silicon crystals have n-type conductivity. As other possible nuclear reactions contribute to a negligible extent, the transmutation nuclear reaction produces n-type semiconductor silicon.

The possibility of doping silicon with phosphorus by neutron irradiation was first pointed out by Lark-Horovitz in 1951[2]. Ten years later, Tanenbaum and Mills[3] carried out the first neutron transmutation doping experiment irradiating small pieces of silicon to study the phosphorus distribution. In the beginning of the seventies, NTD float zone silicon was used for the fabrication of the first high power devices followed by extensive research which demonstrated a clear superiority of the resulting device characteristics [4, 5, 6]. Since then, neutron transmutation doping has been offered by a number of research reactors, mainly in Europe and the USA. The total world production of NTD silicon is estimated to be over 100 tons annually[7] used mainly in the semiconductor industry.

With the increasing demand for NTD silicon with very tight target resistivity tolerances and considering the fact that only a limited number of research reactors are able to irradiate silicon presently, it is important to improve the silicon irradiation process by introducing new procedures and precise neutron dose control methods. The present work describes a very efficient and accurate method of irradiating silicon crystals without the use of neutron absorbing shields or moving the crystals in the axial direction. Radial and axial uniformities, doping accuracy and the simplicity of operation are the main objectives which were considered in the design of a test silicon irradiation facility at IEA-R1 reactor.

## 2. SILICON IRRADIATION RIG

The IEA-R1 reactor is an open swimming pool-type light water reactor operated at 2 MW on an 8 hours a day, 5 days per week, cycle. The reactor core consists of 31 MTR-type fuel elements including 4 elements with neutron absorbing control plates. About half of the fuel elements are 93% <sup>235</sup>U while others use 20% enriched uranium. The reactor core is surrounded by graphite blocks serving as a reflector. A cross-sectional view of the reactor is shown in figure 1. The silicon irradiation position is on the left side top.

Figure 2 is the side view of the silicon irradiation rig which is located in the graphite reflector. The rig essentially consists of two parts, the one fixed on the reactor grid plate is a square cross-sectional aluminium guide tube with dimensions of 12 cm × 12 cm × 150 cm. The other part of the rig consists of a freely rotating cylindrical aluminium tube which

is 175 cm long, has 109 mm internal diameter and 2.5 mm thick wall. The cylindrical tube is supported inside the guide tube through an aluminium pin which holds it at the centre during rotation. The rotating tube is connected to a long aluminium rod which extends above, beyond the pool water, and is coupled to the shaft of an electric motor through a ball bearing. The rotating cylinder serves as the irradiation tube for silicon crystals. The rotation speed is 2 rpm, and to ensure that the tube does in fact rotate during the irradiation period the rotational motion is constantly monitored through an optical sensor.

All the silicon crystals are encapsulated in aluminium cans which are 50 cm tall and have 0.5 mm wall thickness. The internal diameter of the can varies according to the diameter of the silicon crystal to be irradiated (3" or 4"). The aluminium cans are provided with holes at the bottom and at the top to permit the flow of water around the crystal during irradiation.

The neutron dose is measured by two silver wire self-powered neutron detectors (SPND) placed very close to the irradiation tube. The neutron detectors utilize the  $\beta$ -decay of the radioactive silver isotopes  $^{108,110}\text{Ag}$  to produce a current which is proportional to the neutron flux. The current is measured by digital current integrator and counted in a preset scaler. When the integrated counts reach the present value, an alarm sounds prompting the reactor operator to take the necessary action to pull the irradiation tube out of the reactor core. The self-powered neutron detectors are calibrated periodically against cobalt wire monitors irradiated simultaneously. The activity of cobalt monitors is measured by an ionization chamber.

### 3. NEUTRON FLUX PROFILE MEASUREMENT

To obtain the desired resistivity uniformity, the neutron flux must be as homogeneous as possible over the entire crystal volume. While the small radial flux gradient of the reactor can be greatly reduced by rotating the crystal around its axis during the irradiation, which usually results in the radial resistivity variation of the order of 1% or less, the detailed knowledge of the neutron flux variation in the axial direction is essential. The axial flux profile depends on the reactor type and dictates the method to be used for optimizing the maximum to minimum resistivity variation over the ingot length and consequently the maximum ingot length which can be irradiated.

The thermal neutron flux profile has been measured by the activation method. The selected reaction was  $^{59}\text{Co}(n,\gamma)^{60}\text{Co}$  due to the fact that it is almost insensitive to epithermal neutrons and provides an adequate activity for quick measurement by an ionization chamber or HPGe spectrometer.

Cobalt wire monitors wrapped in thin aluminium sheets were positioned at regular distances on the surface of aluminium rods having the same dimensions as the silicon ingots. Aluminium was chosen because of its similarity to silicon with respect to the neutron scattering and absorption cross-sections. Irradiation of the aluminium rods was carried out by following the identical procedure as adopted for the silicon crystals and the data were obtained for cobalt monitors covered with and without cadmium sheets. The neutron fluence was calculated using the Westcott formalism[8]. Most of the correction factors involved cancelled out and the only remaining important factor was the cobalt wire self-shielding to neutrons which was determined in a separate experiment[9] for the used wire. The measured flux profile is shown in figure 3. The cadmium ratio was determined to be  $29.3 \pm 0.6$ .

#### 4. IRRADIATION METHOD

An inspection of the axial neutron flux profile at the silicon irradiation position (fig. 3) shows that the flux peaking occurs at about the geometrical centre of the irradiation tube and that the neutron flux drops rather steeply but quite symmetrically above and below this central position reaching about 50% of the peak value at approximately 25 cm on either side.

A decision to utilize the maximum possible irradiation capacity of the rig as well as the consideration of the cost for NTD irradiation set the goal to irradiate at least 40 cm long silicon crystals in the installed facility. The approach to axial uniformity involving flux profile modification using neutron absorbers was immediately rejected as this method would reduce about 50% of the available flux capacity.

Excellent characteristics of the flux profile at the irradiation position in our reactor has provided us a better solution to achieve the desired axial uniformity without sacrificing the irradiation capacity. In this method two silicon crystals 20 cm long each, are irradiated together in an aluminium can, with their interface adjusted at the maximum flux position inside the irradiation tube. The irradiation tube is rotated about its axis at 2 rpm during irradiation. At precisely 50% of the total necessary dose, the crystals are pulled out of the core and their positions are interchanged as shown in figure 3. The flux profile being symmetrical, the crystals now see almost mirror images of the respective profiles at previous positions. The irradiation then continues till the remaining dose is complete. Precise detection of the 50% fluence is the key to the success of this method. This is accomplished with the help of self powered neutron detectors placed close to the irradiation tube as well as the cobalt wire monitors which are irradiated together with the silicon crystals.

The resistivity,  $\rho$  for n-type silicon containing C atoms per  $\text{cm}^3$  of dopant concentration of phosphorous can be written as:

$$\rho = (C\mu_e q_e)^{-1} \Omega.cm \quad (2)$$

where  $\mu_e$  is the drift mobility of electrons in the crystal lattice ( $\text{cm}^2/\text{V.s}$ ) and  $q_e$  is electronic charge ( $1.602 \times 10^{-19} \text{coulomb}$ ).

The final concentration of  $^{31}\text{P}$  atoms  $C_f$  in the neutron irradiated silicon is given by:

$$C_f = C_i + C_{NTD} \quad (3)$$

where  $C_i$  is the dopant phosphorous concentration in the n-type starting material.  $C_{NTD}$  is equal to the number of atoms of  $^{31}\text{Si}$ , produced by neutron capture in  $^{30}\text{Si}$ , which subsequently decay to  $^{31}\text{P}$  and can be written as:

$$C_{NTD} = N_0 \sigma_c \phi t \quad (4)$$

where  $N_0$  is the number of atoms of  $^{30}\text{Si}$  per  $\text{cm}^3$  in the starting material. For silicon with specific gravity of  $2.33 \text{ g/cm}^3$ , atomic weight of 28.086 and  $^{30}\text{Si}$  isotopic abundance of 3.09%,  $N_0 = 1.544 \times 10^{21} \text{ atoms/cm}^3$ ,  $\sigma_c$  is the neutron capture cross section of  $^{30}\text{Si}$  ( $\text{cm}^2$ ) and  $\phi t$  is the neutron dose ( $\text{n/cm}^2$ ).

Combining equations (2), (3) and (4) the relation between the neutron dose  $\phi.t$  ( $\text{n/cm}^2$ ) received by the silicon crystals and the final resistivity  $\rho_f$  ( $\Omega.cm$ ) attained after irradiation can now be written as:

$$\phi.t = K \left[ \frac{1}{\rho_f} - \frac{1}{\rho_i} \right] \quad (5)$$

where  $\rho_i$  is the initial resistivity of the crystal and,

$$K = (N_0 \sigma_c \mu_e q_e)^{-1}$$

The constant  $K$  ( $\Omega/cm$ ) depends mainly on the neutron capture cross section of  $^{30}\text{Si}$  which in turn is determined by the neutron energy spectrum at the irradiation position and is therefore characteristic of each reactor. Precise experimental determination of the value of  $K$  is essential for the calculation of the required neutron dose to achieve a given target resistivity.

The effective neutron dose received by the silicon crystals during the irradiation was measured by small cobalt wire monitors wrapped in thin aluminium sheets and fixed at the top and at the bottom of each crystal. The irradiation time is controlled by the integrated current signals from two self powered neutron detectors (SPND) fixed very close to the irradiation tube.

After irradiation the aluminium can containing the crystals is removed from the irradiation tube and placed in the pool storage space away from the reactor core. The crystals remain in the storage for about 5 days to permit the decay of  $^{31}\text{Si}$  ( $T_{1/2} = 2.62$  d) and are then removed from the reactor, washed with distilled water, dried and monitored for residual radioactivity.

The doping process produces  $^{32}\text{P}$  inside the silicon crystal through a secondary reaction when  $^{31}\text{P}$  formed in the main transmutation reaction (1) continues to be irradiated with thermal neutrons. The  $^{32}\text{P}$  decays with an emission of  $\beta$  particle and a half-life of 14.6 days. Although it exists in a very small quantity, the activity of this radionuclide must be measured and compared with the exempt limits stated in the IAEA regulations for the safe transport of radioactive material before the crystals can be released for industrial processing. From the regulations, the level of  $^{32}\text{P}$  radioactivity with which the material could be classified as exempt is 7.4 Bq/g.

As the greater portion of the  $\beta$  particles are self absorbed within the crystal, to measure the radioactivity equivalent to 7.4 Bq/g is extremely difficult and it is much easier to relate the radioactivity to the count rate of  $\beta$  particles. This involves careful calibration of the detector system. The  $^{32}\text{P}$  activity is monitored by means of a Geiger-Muller detector which has been adequately calibrated by using a  $^{32}\text{P}$  standard source. Experimental details of the detector calibration are described elsewhere[9].

Each crystal is subject to check by the calibrated G-M detector. Different regions of the crystal surface are monitored separately and the average value is compared with the exempt limit.

## 5. RESULTS AND DISCUSSION

A series of test irradiations were performed with float-zone silicon crystals having diameters of 3 and 4 inches and a length of 20 cm each. The silicon crystals were furnished by a Japanese manufacturer and shipped to our laboratory usually in the lots of 4 to 6 ingots. A total of 100 crystals were irradiated for the test experiments. The initial resistivity of the crystals varied from 1000 to 20000  $\Omega\text{cm}$ , depending on the batch, and the target resistivities varied between 33 to 220  $\Omega\text{cm}$  and specified in each case by the manufacturer. The irradiation of silicon crystals was carried out following the procedure outlined in the preceding section. After irradiation, the crystals of each lot were checked for the residual radioactivity and finally shipped back

to the manufacturer where they were submitted to an appropriate thermal annealing process before measuring the final resistivity. The data on the final resistivity of each crystal in a given lot were furnished by the manufacturer along with the shipment of next lot for the irradiation so that the irradiation parameters could be appropriately adjusted if necessary. The resistivity measurements were carried out on both flat faces of each ingot using a four point probe. The calculations of the axial and radial variation of the resistivity as well as the doping accuracy were made by using the following expressions:

1. axial resistivity variation

$$A = \frac{\bar{\rho}(U)}{\bar{\rho}(L)} \quad (6)$$

where  $\bar{\rho}(U)$  and  $\bar{\rho}(L)$  are the average resistivity values for the upper face (crystal identification number is marked on this face) and the lower face respectively.

2. radial resistivity variation

$$R = \frac{\rho^{max} - \rho^{min}}{\rho^{min}} \times 100 \quad (7)$$

where  $\rho^{max}(\rho^{min})$  are the maximum(minimum) resistivity values for each crystal face.

3. Doping accuracy

$$A_c = \frac{\bar{\rho}}{\rho(T)} \quad (8)$$

where  $\bar{\rho}$  is the average final resistivity and  $\rho(T)$  is the target resistivity.

The results obtained in the test irradiation are shown in figure 4. These results clearly show the excellent doping quality achieved. More than 80% of the crystals show axial variation of the resistivity which is equal or less than 3%. The maximum observed variation in all cases is 5% or less. More than 95% of the crystals attained radial doping uniformity which is equal or less than 2%. In more than 80% of the cases the doping accuracy achieved was better than 3%. These results can be considered entirely satisfactory when compared with the commercially produced NTD silicon in other reactors.

Experimental data obtained in the test irradiations also served to determine a precise value of the calibration constant  $K$  appearing in the equation (5). A least square fit of the data to equation (5) gave, in the case of 4 inch crystals,

$$\phi.t = (2.751 \pm 0.012) \times 10^{19} \left[ \frac{1}{\rho_f} - \frac{1}{\rho_i} \right] n/cm^2 \quad (9)$$

The effective neutron cross section,  $\sigma_c$  obtained by using the above value of  $K$  is  $0.109 \times 10^{-24} \text{ cm}^2$ . The calculated value of the cross section is however somewhat dependent on the used value of the drift mobility of electrons in the crystal,  $\mu_e$ . The literature values of  $\mu_e$  vary between 1220 to 1500  $\text{cm}^2/\text{V.s}$ [10]. The value used in the present calculation was 1350  $\text{cm}^2/\text{V.s}$  taken from reference 10. The value of neutron cross section determined of this manner from NTD data includes phosphorous production from thermal well as epithermal neutrons. This value agrees reasonably well with values reported in the literature for light water reactors which may have measurable production from epithermal neutrons.

A simple design irradiation rig has been constructed and installed in the IEA-R1 research reactor for the neutron transmutation doping of 3 and 4 inch diameter silicon crystals. A reasonably symmetric thermal neutron flux profile at the irradiation position permitted the irradiation of two silicon ingots, each 20 cm long simultaneously. By interchanging the position of ingots at precisely half the required neutron dose, it has been possible to achieve an excellent axial doping uniformity. Test irradiation of 100 silicon crystals demonstrated excellent doping uniformities as well as doping precision.

### Acknowledgement

Parcial financial support for the NTD project was provided by the International Atomic Energy Agency (IAEA) and the Financiadora de Estudos e Projetos (FINEP). Efficient collaboration from the IEA-R1 reactor staff is thankfully acknowledged.

### References

- [1] HERZER, H., "Neutron-doped silicon - A market review", Neutron transmutation doping of silicon (Proc. Int. Conf. Copenhagen, 1980), (GULDBERG, J. Ed), Plenum Press, New York (1981) 1-17.
- [2] LARK-HOROVITZ, K., "Nucleon-bombarded semiconductor", Semi-conducting materials ( Proc. Int. Conf. London, 1951), Butterworth, London, (1951) 47 - 69.
- [3] TANENBAUM, M., MILLS, A. D., Preparation of uniform resistivity n-type silicon by nuclear transmutation, J. Electrochem. Soc. 108 (1961) 171 - 176.
- [4] SCHNÖLLER, M., Breakdown behavior of rectifiers and thyristors made from striation-free silicon, IEEE Trans. Electron. Devices ED-21 (1974) 313 - 314.
- [5] JANUS, H. M., MALMROS, Ö., Application of thermal neutron irradiation for large scale production of homogeneous phosphorous doping of float zone silicon, IEEE Trans. Electron. Devices ED-23 (1976) 797 - 802.
- [6] MEESE, J. M., COWAN, D. L., CHANDRASEKHAR, M., A review of transmutation doping in silicon, IEEE Trans. Nucl. Science NS-26 (1979) 4858 - 4867.
- [7] VON AMMON, W., Neutron transmutation doped silicon - technological and economic aspects. Nucl. Instrum. Meth. Phys. Research B63 (1992) 95 - 100.
- [8] DROULERS, Y. Neutron Fluence Measurements, Technical report series number 107, International Atomic Energy Agency, Vienna, 1970.
- [9] SEBASTIÃO, J. R., Neutron transmutation doping of monocrystalline silicon with phosphorous MSc. Thesis, IPEN, São Paulo (1992). (in Portuguese)
- [10] CRICK, N. W., "The optimisation of nuclear parameters used for silicon irradiation in the Harwell research reactors. Neutron transmutation doping of silicon (Proc. Int. Conf. Copenhagen, 1980), (GULDBERG, J. Ed), Plenum Press, New York (1981) 211 - 221.

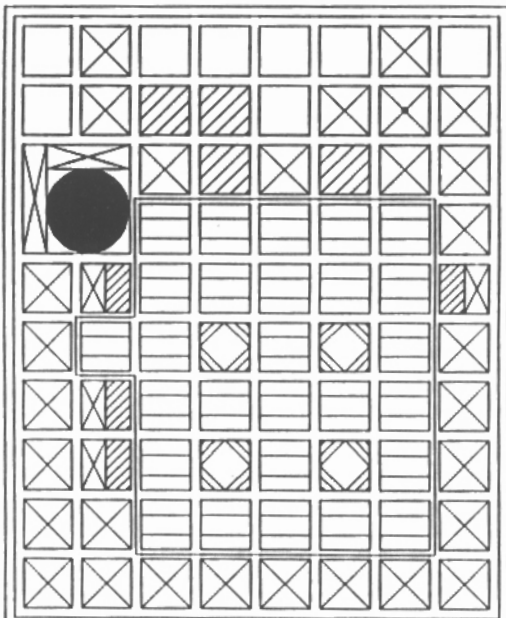
## Figure Captions:

**figure 1.** A Cross-sectional view of the IEA-R1 research reactor core.

**figure 2.** A side view of the silicon irradiation rig located in the graphite reflector.

**figure 3.** Experimentally measured thermal neutron flux profile in the vertical direction (a). The final flux profile as would be seen by the crystal pair when their positions are interchanged at 50% of the required dose (b).

**figure 4.** Results of the test irradiations: Axial resistivity variation (a), Radial resistivity variation (b) and Doping accuracy (c). The quantities  $A$ ,  $R$  and  $A_c$  are as defined in the equations 6, 7 and 8 in the text.



**FUEL  
ELEMENT**



**NEUTRON  
SOURCE**



**NTD  
RIC**



**CONTROL  
ELEMENT**



**BLANK**



**GRAPHITE  
REFLECTOR**



**IRRADIATION  
POSITION**

